New advances in image processing : Some Inverse Problems in Biomedical Imaging

Denis Kouamé

IRIT, Université Toulouse 3 - Paul Sabatier

IRIT - CRCA February 2023

Outline of the talk

Medical imaging modalities

- Nuclear medicine (SPECT, PET)
- Radiology techniques (X-ray radiography, CT, MRI, Ultrasound)

- Scanners

Spatial resolution in medical imaging

- Ultrasound imaging
  - Increase the frequency - trade-off with penetration depth

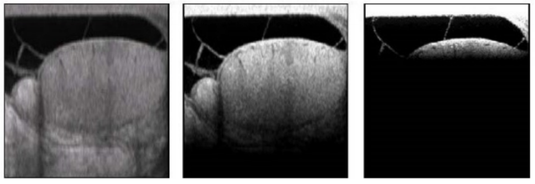

  - Increase the number of fires - trade-off with frame rate

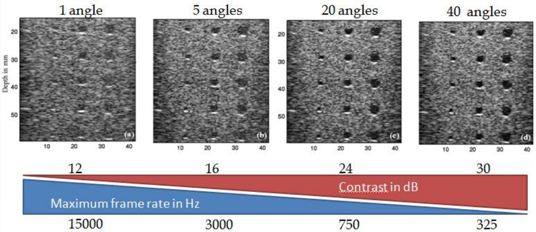

Spatial resolution in medical imaging

- Computed tomography
  - Increase the radiation dose - trade-off with patient danger and acquisition time

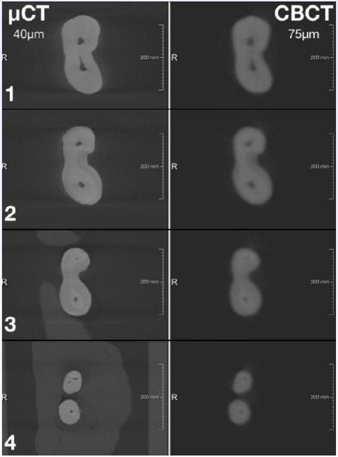

Summary

Spatial resolution in medical imaging

- Instrumentation definitely helps but at the cost of...
  - Field of view
  - Irradiation dose
  - Frame rate
  - Cost
- **Can we (partially) compensate for the loss of spatial resolution with post-processing methods** ?
  - Image restoration seen as an inverse problem
- **This also applies to biological images**

Outline of the talk

Schematic view

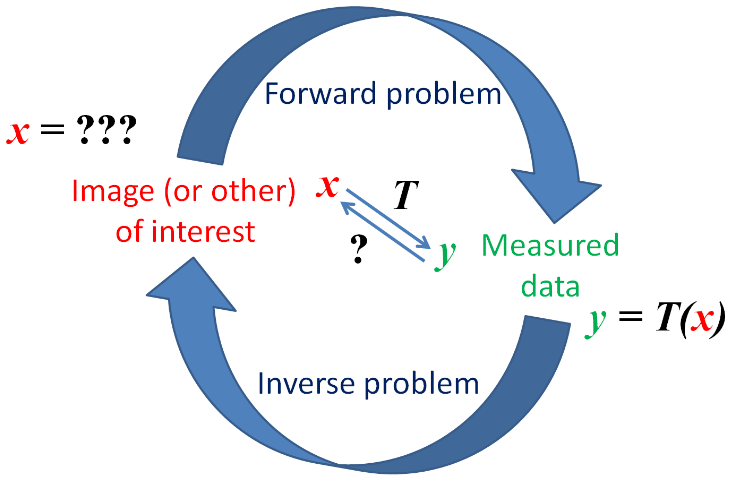

Ill-posedness

$$\mathbf{y} = T(\mathbf{x}) + \mathbf{n}$$

- $\mathbf{y} \in \mathbb{C}^M$ is the observed data (image)
- $\mathbf{x} \in \mathbb{C}^N$ is the image of interest (not observed)
- $\mathbf{n} \in \mathbb{C}^M$ is the noise

T is the observation (forward) operator

- known : estimate $\mathbf{x}$ from $\mathbf{y}$
- unknown : estimate $\mathbf{x}$ and T from $\mathbf{y}$
  - Prior information on T (linear, parametric,...)

Inverse problems in computational medical imaging are usually ill-posed

- T is not invertible
- An infinity of solutions may exist
- A small perturbation on the data may cause an important variation on the estimate (e.g. Fourier measurements)

Outline of the talk

General path

From the forward model to its inversion

- Establish the forward model T linking the unknown (image) to the data
  - Balance between fidelity to physics and computational tractability
- Define proper prior information about $\boldsymbol{x}$ and the noise
  - Important impact on the solution's pertinence
- Formalize the inverse problem as a cost function minimization
- Stochastic simulation or numerical optimization to find the minimizer
  - Convexity of the cost function
  - Form of the forward operator T
  - Continuous and/or discrete variables
- Is the solution reliable ?

Outline of the talk

Image restoration models

$$\mathbf{y} = \mathbf{SHx} + \mathbf{n}$$

- $\mathbf{x} \in \mathbb{R}^N$: image to reconstruct
- $\mathbf{y} \in \mathbb{R}^M$: observable data
- $\mathbf{H} \in \mathbb{R}^{N \times N}$: 2D convolution matrix

Deconvolution

- $\mathbf{S}$: identity matrix ($M = N$)

Super-resolution

- $\mathbf{S}$: subsampling matrix ($M = d^2 N$)

Compressed deconvolution

- $\mathbf{S}$: random subsampling matrix ($M << N$)

Denoising

- $\mathbf{SH} = \mathbf{I}$: identity matrix

Outline of the talk

Application Light Sheet Imaging

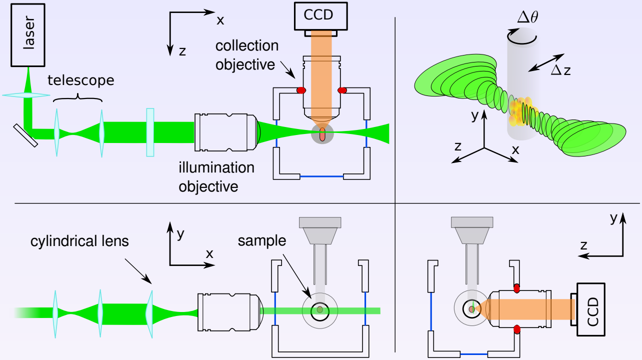

Restoration of light sheet fluorescence microscopy 3D images :

- large 3D images (2Mb per “slice”, usually 300-500 slices)
- optic defects (resolution, blur)
- acquisition noise (low photon emission)

Application Light Sheet Imaging

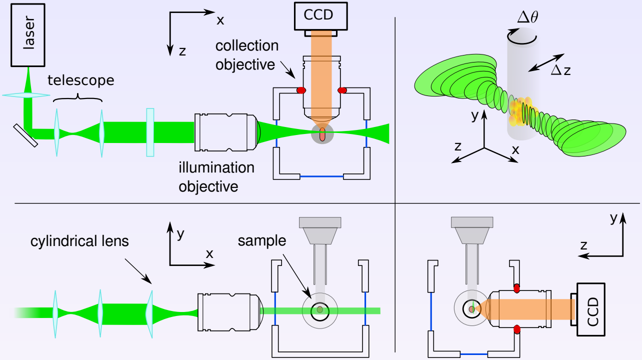

Restoration of light sheet fluorescence microscopy 3D images :

- large 3D images (2Mb per “slice”, usually 300-500 slices)
- optic defects (resolution, blur)
- acquisition noise (low photon emission)

Application Light Sheet Imaging

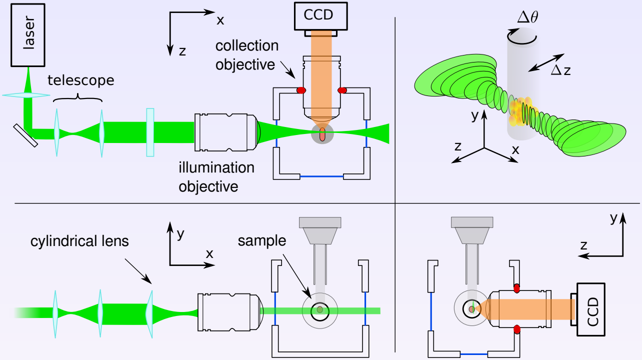

Restoration of light sheet fluorescence microscopy 3D images :

- large 3D images (2Mb per “slice”, usually 300-500 slices)
- optic defects (resolution, blur)
- acquisition noise (low photon emission)

Forward Model

Assuming :

$$\underbrace{m}_{\text{observed data}} = \underbrace{\mathcal{P}}_{\text{Poisson noise}} \left(\underbrace{H}_{\text{convolution matrix}} \underbrace{x}_{\text{unknown data}} \right)$$

With prior :

$$p(x) \propto \prod_{voxels} \exp\left(-\alpha TV(x)\right)$$

Boils down to the unconstrained problem :

$$\arg\min_{x \in \mathbb{R}^n} \langle 1, Hx \rangle - \langle m, \log(Hx) \rangle + \alpha TV(x)$$

Inversion by ADMM

Let $x \in \mathbb{R}^n$, $y \in \mathbb{R}^m$, B a matrix with l rows and n columns, C a matrix with l row and m columns and $b \in \mathbb{R}^l$.

$$\arg \min_{s.t. Bx - Cy = b, x \in X, y \in Y} f_1(x) + f_2(y) \tag{1}$$

$$\begin{aligned}\mathcal{L}(x, y, \lambda) = &< 1, w > - < y, \log(w) > + \alpha \|z\|_1 + \\ &< \lambda, Bx - Cy - b > + \frac{\beta}{2} \|Bx - Cy - b\|_2^2 ,\end{aligned} \tag{2}$$

- $x_{k+1} = \arg\min_{x \in \mathbb{R}^n} \mathcal{L}(x, y_k, \lambda_k)$,
- $y_{k+1} = \arg\min_{y \in \mathbb{R}^m} \mathcal{L}(x_{k+1}, y, \lambda_k)$,
- $\lambda_{k+1} = \lambda_k + \beta(Bx + Cy - b)$,

until stopping criteria are met.

In practice

$$x_{k+1} = \mathcal{F}^{-1}\left(\frac{\mathcal{F}\left(H^T(w_k - \frac{\lambda_{1,k}}{\beta}) + \nabla^T\left(z_k - \frac{(\lambda_{2,k},\lambda_{3,k},\lambda_{4,k})}{\beta}\right)\right)}{\mathcal{F}\left(H^T H + \nabla^T\nabla\right)}\right). \quad (3)$$

$$w_{k+1} = \frac{q - \frac{1}{\beta}}{2} + \frac{1}{2}\sqrt{\left(\frac{1}{\beta} - q\right)^2 + \frac{4m}{\beta}}, \quad (4)$$

$$z_{k+1} = soft_{\frac{\alpha}{\beta}}\left(\nabla x_{k+1} + \frac{(\lambda_{2,k}, \lambda_{3,k}, \lambda_{4,k})}{\beta}\right). \quad (5)$$

With $q = Hx_{k+1} + \frac{\lambda_{1,k}}{\beta}$ and $soft_\gamma(u) \equiv \frac{u}{\|u\|_1} \times max(\|u\|_1 - \gamma, 0)$.

F. de Vieilleville, P. Weiss, V. Lobjois and D. Kouamé, Alternating Direction Method of Multipliers Applied to 3D Light Sheet Fluorescence Microscopy Image Deblurring Using GPU Hardware, *IEEE EMBC*'11.

Drosophila

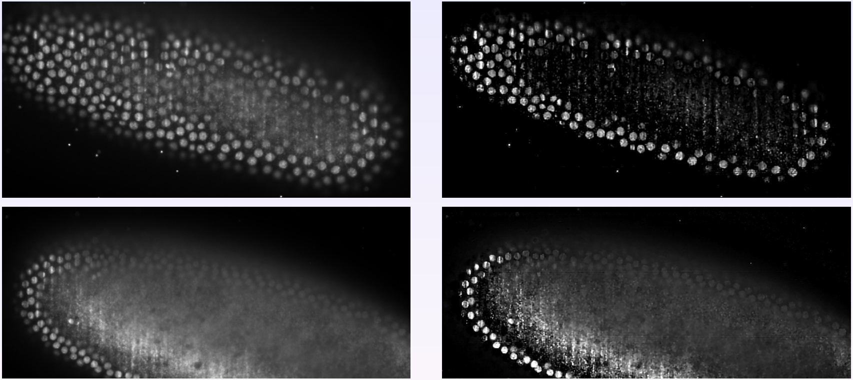

$\alpha = 0.002$, $\beta = 0.002$, 50 iterations.

Spheroids

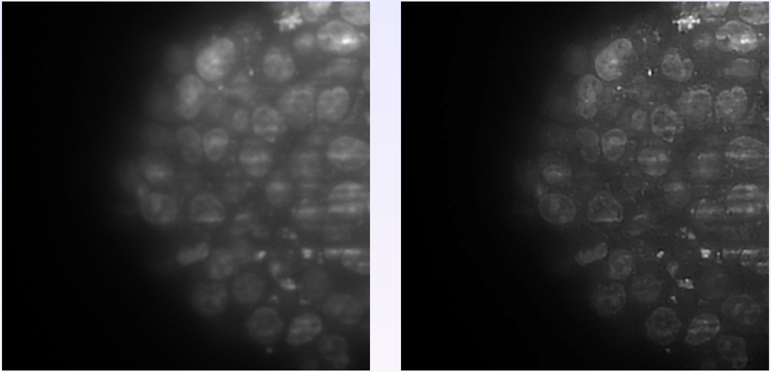

$\alpha = 0.002$, $\beta = 0.002$, 50 iterations.

Outline of the talk

Forward model

$$\mathbf{y} = \mathbf{SHx} + \mathbf{n}$$

- $\mathbf{y} \in \mathbb{R}^{N_l \times 1}$: is the measured image, $N_l = m_l \times n_l$
- $\mathbf{x} \in \mathbb{R}^{N_h \times 1}$: super-resolved image to be estimated, $N_h = d^2 N_l$
- $\mathbf{n} \in \mathbb{R}^{N_l \times 1}$: Gaussian noise

Degradation operators

- $\mathbf{H} \in \mathbb{R}^{N_h \times N_h}$: 2D circulant convolution matrix (PSF of the transducer)
- $\mathbf{S} \in \mathbb{R}^{N_l \times N_h}$: subsampling operator

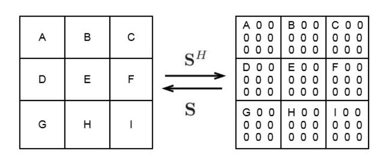

Proposed closed-form solution

$$\min_{\mathbf{x}} \frac{1}{2}\|\mathbf{y} - \mathbf{SHx}\|_2^2 + \tau\|\mathbf{Ax} - \mathbf{v}\|_2^2$$

- Lemma

$$\mathbf{FS}^H\mathbf{SF}^H = \frac{1}{d^2}(\mathbf{J}_d \cdot \mathbf{I}_{m_l}) \cdot (\mathbf{J}_d \cdot \mathbf{I}_{n_l})$$

where $\mathbf{J}_d \in \mathbb{R}^{d\times d}$ is a matrix of ones, $\mathbf{I}_{m_l}$ and $\mathbf{I}_{n_l}$ are identity matrices and $\cdot$ is the Kronecker product.

- Proposed solution $\mathcal{O}(N_h \log N_h)$

$$\hat{\mathbf{x}} = \frac{1}{2\tau}\mathbf{F}^H\mathbf{\Psi}\mathbf{Fr} - \frac{1}{2\tau}\mathbf{F}^H\mathbf{\Psi}\underline{\mathbf{\Lambda}}^H\left(2\tau d\mathbf{I}_{N_l} + \underline{\mathbf{\Lambda}}\mathbf{\Psi}\underline{\mathbf{\Lambda}}^H\right)^{-1}\underline{\mathbf{\Lambda}}\mathbf{\Psi}\mathbf{Fr}$$

where $\mathbf{r} = \mathbf{H}^H\mathbf{S}^H\mathbf{y} + 2\tau\mathbf{A}^H\mathbf{v}$, $\mathbf{\Psi} = \mathbf{F}\left(\mathbf{A}^H\mathbf{A}\right)^{-1}\mathbf{F}^H$ and $\underline{\mathbf{\Lambda}} \in \mathbb{C}^{N_l\times N_h}$ is block diagonal

N. Zhao, Q. Wei, A. Basarab, N. Dobigeon, D. KouamÃľ, J.-Y. Tourneret, Fast Single Image Super-resolution using a New Analytical Solution for ℓ_2-ℓ_2 Problems, *IEEE TIP*, 2016

Super-resolution result on *in vivo* data

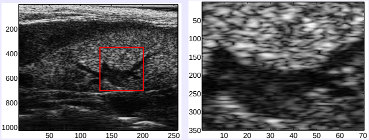

(a) Mouse kidney (b) Observation

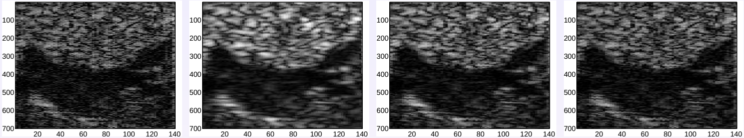

(c) Proposed (ℓ_1) (d) Proposed (ℓ_2) (e) Proposed ($\ell_{1.5}$) (f) Proposed ($\ell_{4/3}$)

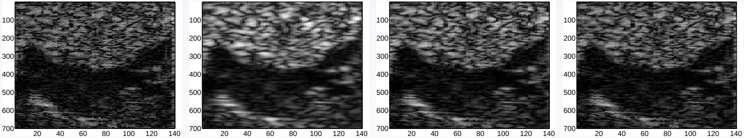

(g) Classical (ℓ_1) (h) Classical (ℓ_2) (i) Classical ($\ell_{1.5}$) (j) Classical ($\ell_{4/3}$)

Outline of the talk

SR for Quantitave acoustic microscopy

Basics of acoustic microscopy

- Very high frequency : 250 and 500 MHz
- Transmits short ultrasound pulses
- Receives the RF echo signals reflected from the sample

Sample

- Thin section of soft tissue (12μm) affixed to a microscopy slide

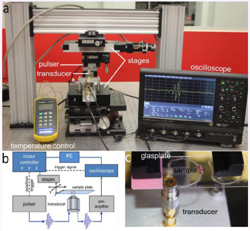

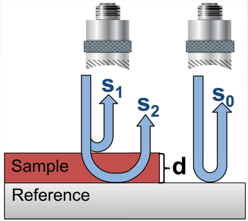

Spatial resolution in acoustic microscopy

Dependent on the central frequency

- Increasing the frequency comes with
  - Increased costs associated with the transducer and then ecessary electronics
  - Experimental difficulties also arise (e.g., sensitivity to nm scale vibrations and temperature)

Example of impedance images on a section of cancerous human lymph node

- Thin section of soft tissue (12μm) affixed to a microscopy slide

250MHz

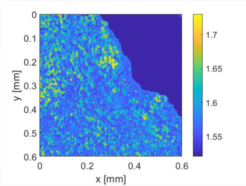

500MHz

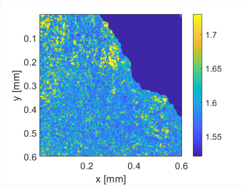

Model-based super-resolution

USAF 1951 resolution phantom

- Super-resolution factor d = 2

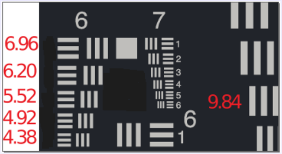

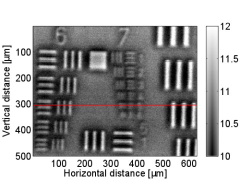

Horizonthal profile

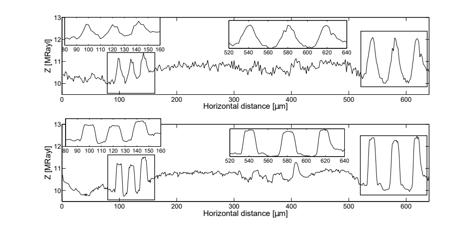

Model-based super-resolution

Fails on ex vivo samples

- Convolution with the PSF not sufficient to model the 250 MHz images

250 MHz　　500 MHz　　Enhanced 250 MHz

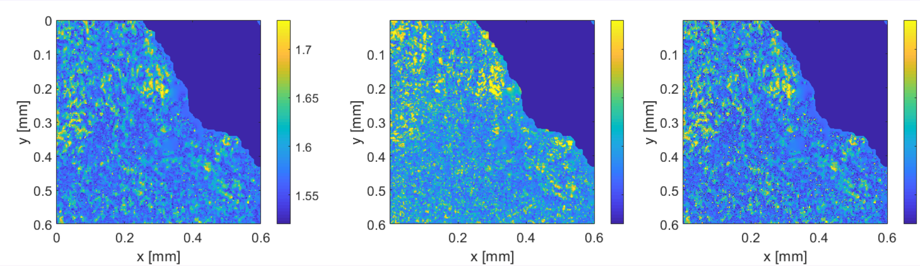

Data-driven super-resolution

Fully convolution neural network (U-net) trained on 250 and 500 MHz images

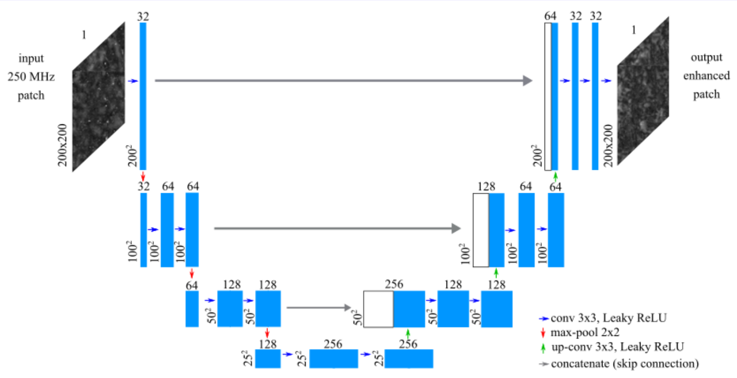

J. Mamou, T. Pellegrini, D. KouamÃľ, A. Basarab, A convolutional neural network for 250-MHz quantitative acoustic-microscopy resolution enhancement,*IEEE EMBC*, 2019.

Results

250 MHz | 500 MHz | Enhanced 250 MHz

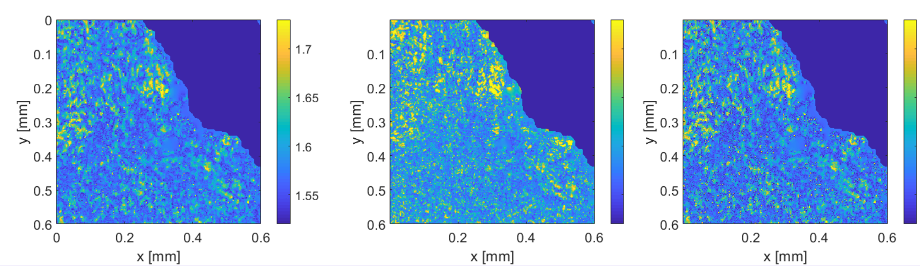

Model-based vs Data driven approach

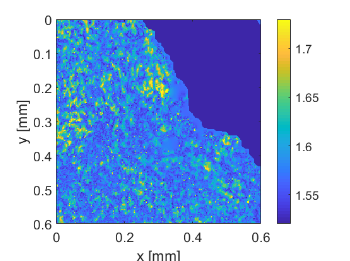

Outline of the talk

Introduction

Background

- The contours of the tumor is important during surgery because it is an area from which the tumor recurs.
- Existing techniques do not allow to precisely visualize this area.

$$\Downarrow$$

"ElastoGli" project

- To characterize in vivo the elasticity and perfusion of the cerebral gliomas and this peritumoral zone.

Photographed by Chloe, another intern at the INSERM.

Data Pre-processing

Casorati matrix

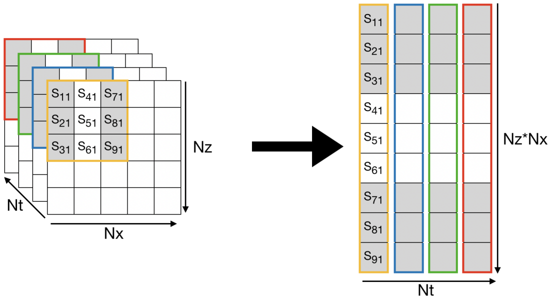

FIGURE: The construction of the Casorati matrix S from a 3D data block

$$data_{(N_z, N_x, N_t)} \Longrightarrow S_{(N_z \times N_x, N_t)}$$

- Axis N_z : the propagation direction of the ultrasound ;
- Axis N_x : the opening of the ultrasound array ;
- Axis N_t : the acquisition of 2D ultrasound plans.

The inversion algorithm

Model Set-up

RPCA : A method to find the optimal sparse (Blood) and low rank (Tissue) estimation from the sequences converted to Casorati matrix, by solving a simple convex estimation problem.

$$\boldsymbol{S} = \boldsymbol{T} + \boldsymbol{B} + \boldsymbol{N}$$

- $\boldsymbol{S} \in \mathbb{C}^{N_z N_x \times N_t}$ is the Casorati matrix obtained from the experimental 3D Doppler data with depth N_z, probe width N_x and acquisition time N_t ;
- $\boldsymbol{T} \in \mathbb{C}^{N_z N_x \times N_t}$, $\boldsymbol{B} \in \mathbb{C}^{N_z N_x \times N_t}$ and $\boldsymbol{N} \in \mathbb{C}^{N_z N_x \times N_t}$ the tissue, blood and noise respectively.

Inversion

$$(\hat{\boldsymbol{B}}, \hat{\boldsymbol{T}}) = \arg\min_{\boldsymbol{B},\boldsymbol{T}} ||\boldsymbol{S} - \boldsymbol{H_1}\boldsymbol{B} - \boldsymbol{H_2} bmT||_F^2 + \lambda||\boldsymbol{B}||_1 + ||\boldsymbol{T}||_*$$

$$\Downarrow$$

ISTA algorithm (could also be done by ADMM)

Iterations

- two main steps

$$\mathbf{L}^{k+1} = \mathrm{SVT}_{\lambda_1/L_f}\left\{\left(\mathbf{I} - \frac{1}{L_f}\mathbf{H}_1^H\mathbf{H}_1\right)\mathbf{L}^k - \mathbf{H}_1^H\mathbf{H}_2\mathbf{S}^k + \mathbf{H}_1^H\mathbf{D}\right\}$$
$$\mathbf{S}^{k+1} = \mathcal{T}_{\lambda_2/L_f}\left\{\left(\mathbf{I} - \frac{1}{L_f}\mathbf{H}_2^H\mathbf{H}_2\right)\mathbf{S}^k - \mathbf{H}_2^H\mathbf{H}_1\mathbf{L}^k + \mathbf{H}_2^H\mathbf{D}\right\}$$

Oren Solomon, Regev Cohen, Yi Zhang, Yi Yang, He Qiong, Jianwen Luo, Ruud J.G. van Sloun, and Yonina C. Eldar, Deep Unfolded Robust PCA with Application to Clutter Suppression in Ultrasound, IEEE Trans. Med. Imging,2020

ISTA algorithm (could also be done by ADMM)

Iterations

- two main steps

$$\mathbf{L}^{k+1} = \mathrm{SVT}_{\lambda_1/L_f}\left\{\left(\mathbf{I} - \frac{1}{L_f}\mathbf{H}_1^H\mathbf{H}_1\right)\mathbf{L}^k - \mathbf{H}_1^H\mathbf{H}_2\mathbf{S}^k + \mathbf{H}_1^H\mathbf{D}\right\}$$
$$\mathbf{S}^{k+1} = \mathcal{T}_{\lambda_2/L_f}\left\{\left(\mathbf{I} - \frac{1}{L_f}\mathbf{H}_2^H\mathbf{H}_2\right)\mathbf{S}^k - \mathbf{H}_2^H\mathbf{H}_1\mathbf{L}^k + \mathbf{H}_2^H\mathbf{D}\right\}$$

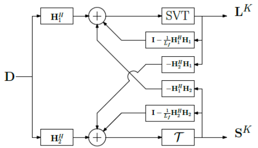

(a) Iterative algorithm for sparse and low-rank separation.

Oren Solomon, Regev Cohen, Yi Zhang, Yi Yang, He Qiong, Jianwen Luo, Ruud J.G. van Sloun, and Yonina C. Eldar, Deep Unfolded Robust PCA with Application to Clutter Suppression in Ultrasound, IEEE Trans. Med. Imging,2020

Deep Unfolded version

Convolution come in the iterations

- Thus,

$$\mathbf{L}^{k+1} = \mathrm{SVT}_{\lambda_1^k}\left\{\mathbf{P}_5^k * \mathbf{L}^k + \mathbf{P}_3^k * \mathbf{S}^k + \mathbf{P}_1^k * \mathbf{D}\right\},$$
$$\mathbf{S}^{k+1} = \mathcal{T}_{\lambda_2^k}\left\{\mathbf{P}_6^k * \mathbf{L}^k + \mathbf{P}_4^k * \mathbf{S}^k + \mathbf{P}_2^k * \mathbf{D}\right\},$$

Oren Solomon, Regev Cohen, Yi Zhang, Yi Yang, He Qiong, Jianwen Luo, Ruud J.G. van Sloun, and Yonina C. Eldar, Deep Unfolded Robust PCA with Application to Clutter Suppression in Ultrasound, IEEE Trans. Med. Imging,2020

Deep Unfolded version

Convolution come in the iterations

- Thus,

$$\mathbf{L}^{k+1} = \mathrm{SVT}_{\lambda_1^k}\left\{\mathbf{P}_5^k * \mathbf{L}^k + \mathbf{P}_3^k * \mathbf{S}^k + \mathbf{P}_1^k * \mathbf{D}\right\},$$
$$\mathbf{S}^{k+1} = \mathcal{T}_{\lambda_2^k}\left\{\mathbf{P}_6^k * \mathbf{L}^k + \mathbf{P}_4^k * \mathbf{S}^k + \mathbf{P}_2^k * \mathbf{D}\right\},$$

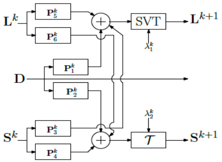

(b) Single layer from the corresponding unfolded algorithm.

Oren Solomon, Regev Cohen, Yi Zhang, Yi Yang, He Qiong, Jianwen Luo, Ruud J.G. van Sloun, and Yonina C. Eldar, Deep Unfolded Robust PCA with Application to Clutter Suppression in Ultrasound, IEEE Trans. Med. Imging,2020

Some results

Classical vs unfolded

- Illustrations,

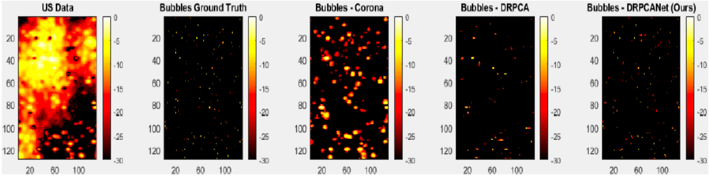

	Corona	DRPCA	Deconvolved Corona	Unfolded DRPCA (Ours)
PSNR (dB)	24.41	27.41	17.85	36.79
SSIM3	0.13	0.49	0.14	0.95

- Some more illustrations

Oren Solomon, Regev Cohen, Yi Zhang, Yi Yang, He Qiong, Jianwen Luo, Ruud J.G. van Sloun, and Yonina C. Eldar, Deep Unfolded

Outline of the talk

Hamiltonian operator

- Construct an adaptive basis using the solutions of SchrÃűdinger equation.
- The Schroedinger equation :

$$-\frac{\hbar^2}{2m}\nabla^2\psi = -V(a)\psi + E\psi$$

- Can be rewritten as an eigenvalue problem :

$$\boldsymbol{H}_{\mathcal{QAB}}\psi = E\psi,$$

  where $\boldsymbol{H}_{\mathcal{QAB}} = -\frac{\hbar^2}{2m}\nabla^2 + V$ is the Hamiltonian operator.
- Main idea : replace $V(a)$, the potential of the system, by an image pixels' values.
- The Hamiltonian operator associated to an image

$$\boldsymbol{H}_{\mathcal{QAB}}[i,j] = \begin{cases} \boldsymbol{x}[i] + 4\frac{\hbar^2}{2m} & \textit{for } i = j, \\ -\frac{\hbar^2}{2m} & \textit{for } i = j \pm 1, \\ -\frac{\hbar^2}{2m} & \textit{for } i = j \pm n, \\ 0 & \textit{otherwise}, \end{cases}$$

Quantum adaptive transform

- The set of eigenvectors corresponding to the Hamiltonian operator represents the adaptive transform and is denoted as the quantum adaptative basis (QAB).

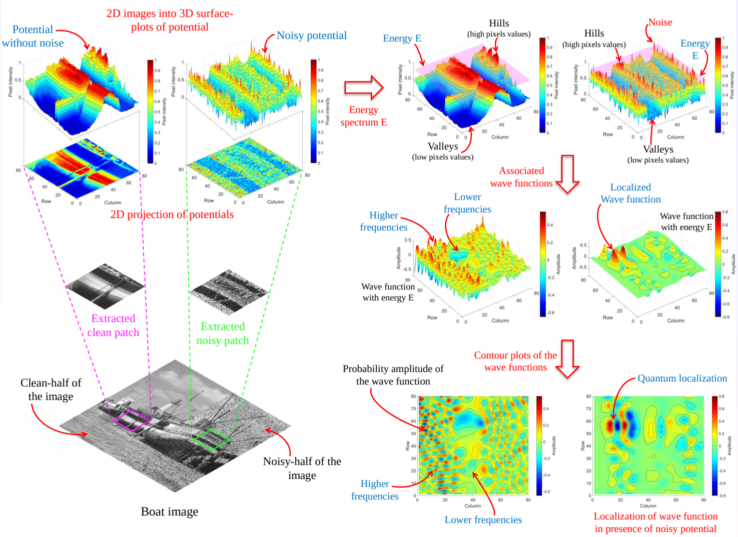

Denoising results

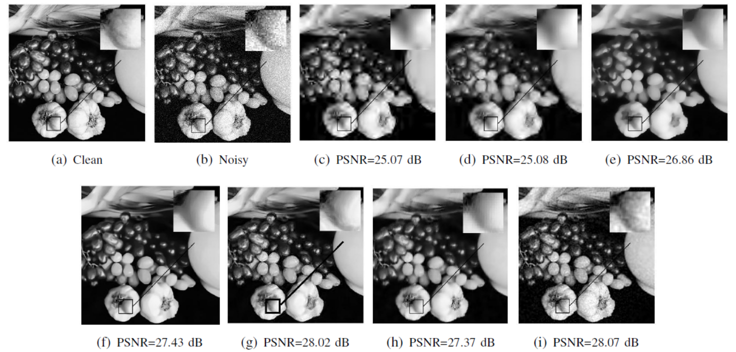

- (a) Clean Fruits image, (b) Image corrupted with Gaussian noise corresponding to a SNR of 15 dB.
- Denoising results obtained using : (c) wavelet hard thresholding, (d) wavelet soft thresholding, (e) total variation regularization, (f) graph signal processing, (g) non-local means, (h) dictionary learning and (i) proposed method.

TDeep unfolding

The architecture of the proposed Deep-Quantum-based image denoising

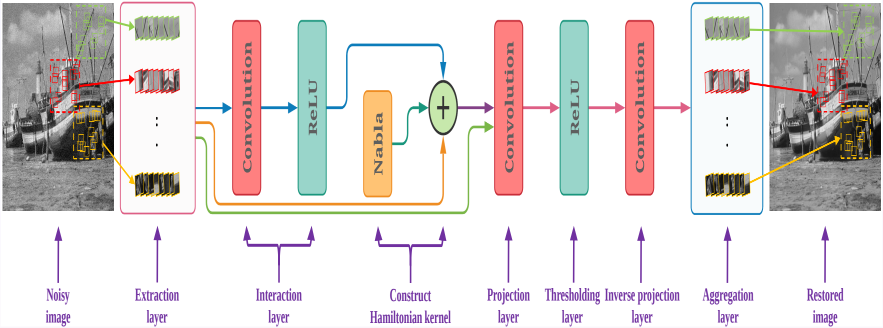

Some results

Classical vs unfolded

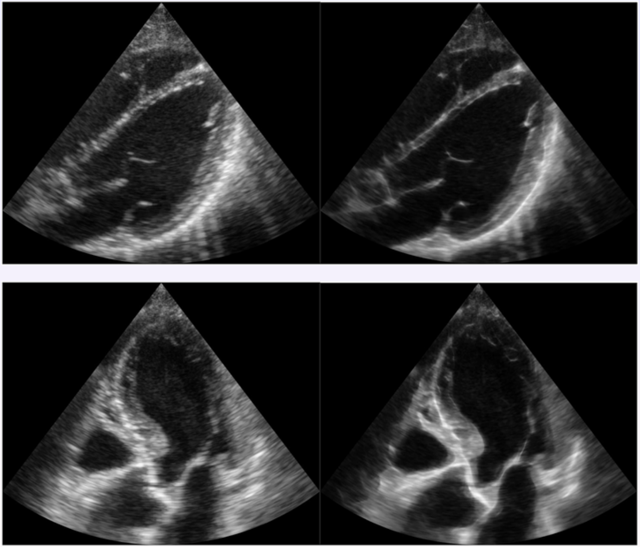

New advances in image processing : Some Inverse Problems in Biomedical Imaging

Denis Kouamé

IRIT, Université Toulouse 3 - Paul Sabatier

IRIT - CRCA February 2023